

Canadian developments in the application of superconducting magnets for levitation, synchronous propulsion, and guidance of high speed inter-city ground transport are described. At  $480 \text{ km h}^{-1}$  a 100 passenger vehicle weighing  $300 \text{ kN}$  is levitated  $15 \text{ cm}$  clear of a flat guideway (minimizing ice and snow accumulation) by eight  $3.85 \times 10^5$  ampere-turns  $100 \times 30 \text{ cm}$  magnets interacting with eddy currents induced in two  $80 \times 1 \text{ cm}$  aluminium strips. The variable speed LSM uses fifty  $5 \times 10^5$  ampere-turns  $40 \times 150 \text{ cm}$  magnets interacting with split three-phase windings energized in  $5 \text{ km}$  sections and phase angle controlled to give 72% efficiency and 0.82 power factor. A lateral restoring force of  $10^4 \text{ N cm}^{-1}$  is produced by the propulsion magnets interacting with the levitation strip edges and with flat null-flux loops overlying the LSM windings. A review of cryogenic systems indicates that isochoric dewar operation is best suited for Maglev vehicles. The test facility, using stationary full-scale superconducting magnets and guideway components mounted on a  $100 \text{ km h}^{-1}$  vertical axis  $7.6 \text{ m}$  diameter wheel, is now fully operational and LSM tests are being performed.

## Canadian developments in superconducting Maglev and linear synchronous motors

D. L. Atherton and A. R. Eastham

Analysis of current and projected transit modes between Toronto and Montreal shows that  $400\text{--}500 \text{ km h}^{-1}$  guided ground transport can be very competitive with short haul air transport with regard both to travelling time and energy consumption. Fig.1 compares total travel times, including entering and leaving the terminal and waiting times for a typical business trip between city centres in Toronto and Montreal. The appeal of short take-off and landing (STOL) aircraft, operating from sites close to the city centre, and high speed guided ground transport (HSGGT), such as Maglev, is readily apparent. The two modes can be complementary as STOL is best suited to short hop, low passenger density operations, while potentially high passenger densities are required for a HSGGT system.

Population density in the Canadian corridor (Toronto—Ottawa—Montreal) is at present only 15% of that in Japan (Tokyo—Osaka), in North-East USA (Boston—New York—Washington) or along routes in Western Europe (such as Hamburg—Munich). We therefore expect that Canadian applications for HSGGT will be later than in these countries.

Superconducting Maglev and linear synchronous motor (LSM) propulsion for high speed inter-city transportation is being investigated by the Canadian Maglev Group, an interdisciplinary team of scientists and engineers from Queen's University, the University of Toronto, and McGill University, under the administration of the Canadian Institute of Guided Ground Transport at Queen's University. Our present development programme is modest compared with efforts in Japan and West Germany, but stresses some relatively advanced concepts, including variable speed phase angle controlled LSM propulsion and guidance schemes using flat-topped guideways (minimizing ice and snow accumulation—a potentially serious problem during Canadian winters).

The authors are in the Physics Department, Queen's University, Kingston, Ontario K7L 3N6, Canada. Received 25 March 1975.

### The Maglev system

A cross-section and plan of the proposed vehicle and guideway are shown in Figs 2 and 3. The vehicle is levitated  $15 \text{ cm}$  clear of a flat guideway by electrodynamic suspension, generated by the interaction of vehicle-borne superconducting magnets and eddy currents induced in aluminium strips or ladders in the guideway. Propulsion and control is by variable frequency LSM; vehicle-borne superconducting 'field' magnets are locked into a travelling magnetic wave produced by powered three-phase stranded aluminium 'armature' windings along the guideway. The vehicle is guided by the vehicle-borne propulsion magnets interacting with the inner edges of the

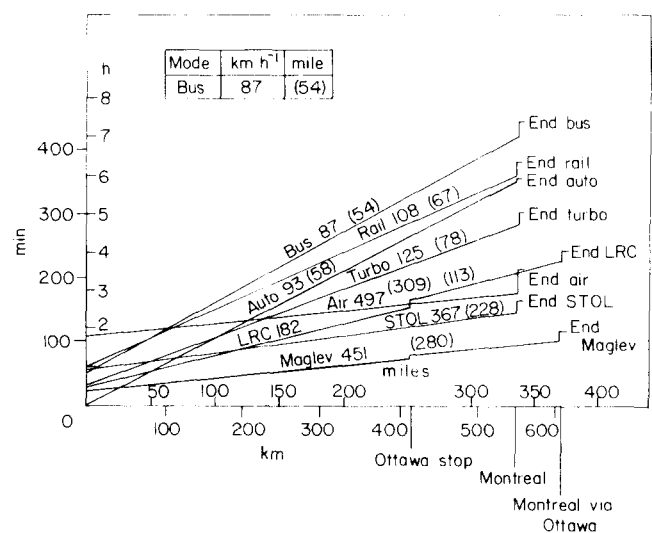


Fig.1 Time versus distance for a typical Toronto—Montreal business trip (door-to-door) by different transit modes. Average vehicle speeds are shown in  $\text{km h}^{-1}$  (and  $\text{mile h}^{-1}$ ). Maglev and LRC (advanced rail) trips include a stop at Ottawa

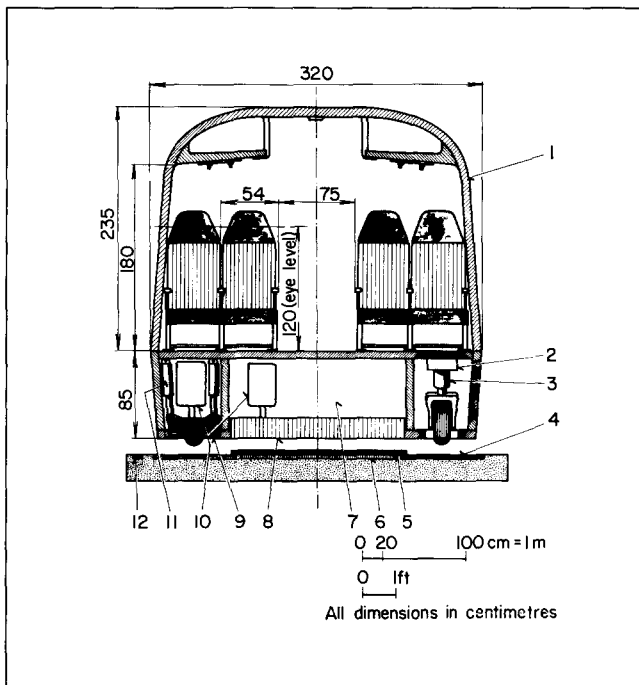


Fig.2 Cross-section of the proposed Maglev vehicle and guideway  
 1 — structure; 2 — automatic low-speed steering device; 3 — retractable wheel for low speed suspension; 4 — aluminium guideway surface for levitation; 5 — guidance coils; 6 — linear synchronous motor windings; 7 — air conditioner, batteries, storage, etc; 8 — propulsion superconducting magnet; 9 — levitation superconducting magnet; 10 — isochoric liquid helium reservoir; 11 — secondary suspension; 12 — vehicle detector

levitation strips and with flat null-flux loops mounted along the centre of the guideway.

Parameters for the Canadian Maglev system are given in Table 1. It will be noted that the use of electrodynamic suspension and LSM propulsion allows very lightweight vehicles. A 100 passenger capacity Maglev vehicle is estimated to weigh 300 kN compared with 500 kN for a tracked air cushion vehicle of similar capacity. The reduced guideway loading, together with the large guideway clearance of 15 cms at high speed (allowing normal civil engineering tolerances), minimizes the cost of guideway construction (which is the dominant factor in any system cost).

Aerodynamic forces impose a limit to the maximum operational cruising speed over an open guideway. At 480 km h<sup>-1</sup>, aerodynamic drag accounts for over 70% of the total drag force on the vehicle, while crosswinds produce large side forces (70 kN in a 100 km h<sup>-1</sup> crosswind).

The short duration, radiated boundary layer noise from a high speed Maglev vehicle is estimated to be 89 dbA at a 15 m side-line, that is, no more than that from an average highway. Noise at low speed in urban areas is minimal. An internal noise level of 80 dbA at 480 km h<sup>-1</sup> is anticipated, requiring the extensive use of sound absorbent materials in interior design.

The estimated energy efficiency of Maglev, in terms of passenger miles per unit energy is compared with that for other inter-city modes in Fig.4. In relation to total door-to-door travelling time, HSGGT modes make more efficient use of the high energy consumption common to any high speed system.

The Maglev system itself is pollution-free. The LSM is an efficient means of propulsion and uses electrical energy, centrally generated from hydro, nuclear fuels, etc (rather than using a particular depletable fossil fuel).

### Levitation

Our major efforts have been devoted to analysis and modelling of continuous strip guideways, although we are also investigating possible ladder configurations. A preliminary technical and economic analysis of the levitation system has been performed in an attempt to determine the optimum vehicle magnet configuration and guideway strip thickness.

Magnet dimensions have been optimized with respect to a wide range of parameters. From considerations of ampere-turns, stored energy, cost, efficiency, variation of lift with speed, low speed drag forces, and magnetic fields in the passenger compartment, a large square coil is preferred. However, to minimize capital investment in guideway aluminium, a narrow coil is required. An engineering/economic compromise results in the selected levitation coils being 1.0 m long x 0.3 m wide and

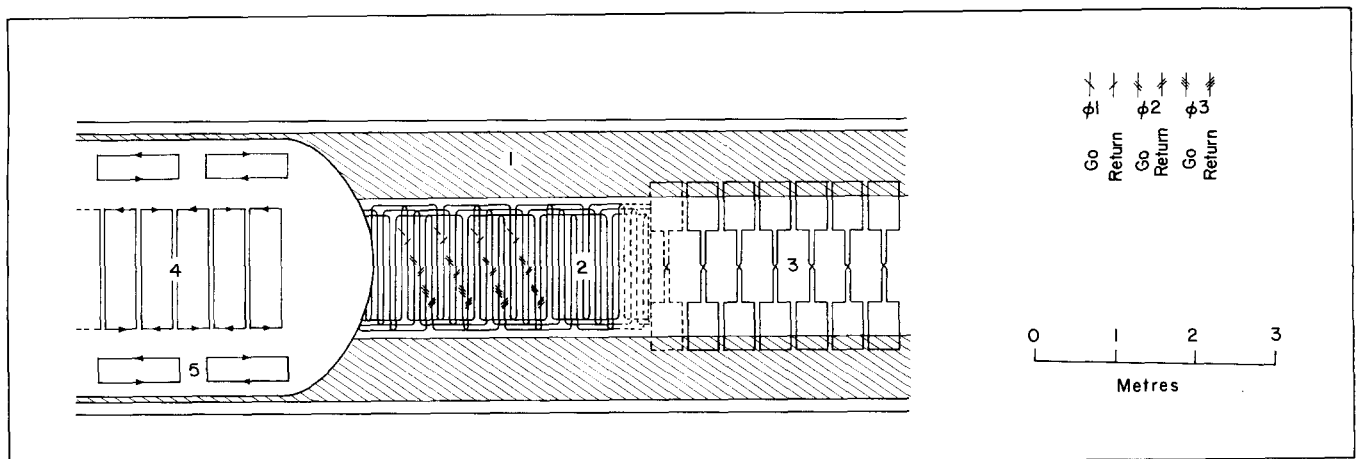


Fig.3 The proposed layout of vehicle magnets and guideway conductor configuration for the Canadian Maglev system  
 1 — aluminium levitation strip; 2 — linear synchronous motor windings; 3 — null-flux guidance loops; 4 — superconducting propulsion magnets; 5 — superconducting levitation magnets

**Table 1. Canadian superconductive Maglev system parameters**

Vehicle	
Speed	480 km h <sup>-1</sup>
Estimated laden weight	300 kN (30 tonnes)
Length	35 m
Width	3.2 m
Height	3.2 m
Passenger capacity	100
Ground clearance	15 cm
Predicted aerodynamic drag at 480 km h <sup>-1</sup>	29 kN
Suspension	
No of superconducting magnets	8
Strength	3.85 x 10 <sup>5</sup> ampere turns
Size	1.0 m long x 0.3 m wide
Mean suspension height	22 cm
Magnetic drag at 480 km h <sup>-1</sup>	11 kN
Suspension stiffness	3 x 10 <sup>6</sup> N m <sup>-1</sup>
Natural frequency	1.6 Hz
Sprung secondary suspension with active damping by LSM	
Propulsion	
Linear synchronous motor (3 phase)	
No of superconducting magnets	50
Strength	5 x 10 <sup>5</sup> ampere turns
Size	0.4 m long x 1.5 m wide
Pitch	45 cm
Nominal power	5.2 MW
Thrust	40 kN
Guideway section length	5 km
Conductor cross-section	0.8 cm <sup>2</sup>
Efficiency	72%
Power factor	0.82
Guideway	
Elevated flat-topped concrete beam	
Width	3.7 m
Levitation strips	2, each 1 cm thick x 80 cm wide
Guidance	
Pitch of 'null-flux' loops	37.5 cm
Conductor cross-section	3 cm <sup>2</sup>
Predicted lateral load due to 100 km h <sup>-1</sup> sidewind	70 kN
Lateral stiffness	10 <sup>6</sup> N m <sup>-1</sup>
Maximum restoring force	280 kN
Lateral natural frequency	0.91 Hz

having 3.85 x 10<sup>5</sup> ampere-turns. Eight magnets are required to lift an estimated vehicle weight of 300 kN.

The effect of strip width on the high speed lift force has been investigated by modelling the electrodynamic suspension by a full-scale ac excited copper coil positioned over aluminium strips of various width.<sup>2,3</sup> The results of impedance measurements, given in Fig.5, show that there is no appreciable degradation of lift force for strip widths down to 50 cms (for a 30 cm wide magnet).

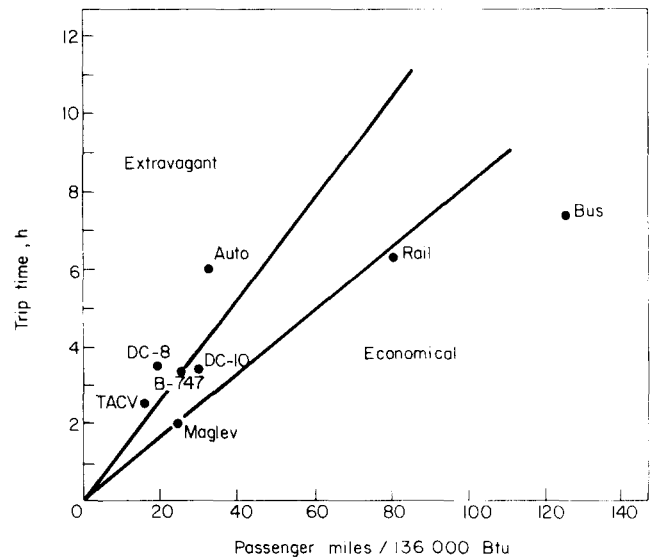


Fig.4 The energy efficiency of various inter-city transit modes. Typical door-to-door times for a business trip (Toronto-Montreal) as a function of passenger miles per 136 000 Btu. For Maglev, a load factor of 0.6, motor efficiency of 70%, conversion efficiency of 85%, and generation and distribution efficiency of 30% is assumed

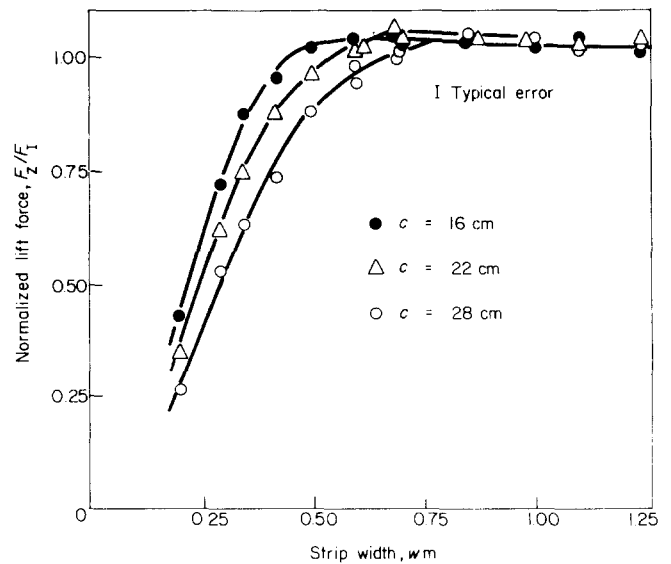


Fig.5 The high speed lift force determined by impedance modelling, normalized to the calculated full image force, as a function of strip width for various levitation heights

However, the operational strip width is set primarily from considerations of the destabilizing force acting when the magnets (and vehicle) are displaced off-centre.<sup>4</sup> The magnitude of this force, again determined by impedance modelling, is shown in Fig.6 for strip widths of 60 cm and 100 cm. A 100 km h<sup>-1</sup> side wind is estimated to produce a 70 kN side force on the Maglev vehicle and, for a specified guidance stiffness of 10<sup>6</sup> N m<sup>-1</sup>, would produce a lateral displacement of 7 cm. In order to keep the resultant lateral destabilizing force small, a levitation strip width of 80 cm is selected.

Finite strip width effects have also been investigated by measuring the induced eddy current distribution across strips of various widths (again by ac modelling<sup>3</sup>). The

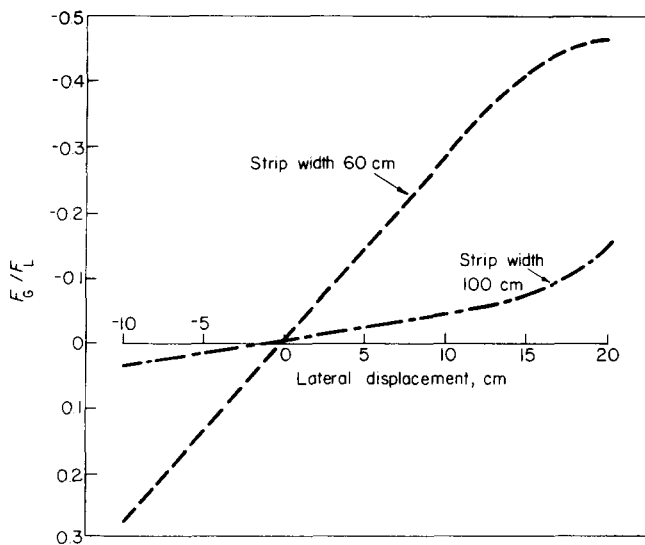


Fig. 6 The lateral destabilizing force on a 100 cm long x 30 cm wide magnet determined by impedance modelling, normalized to the lift force at zero offset, as a function of lateral displacement over levitation strips of different widths

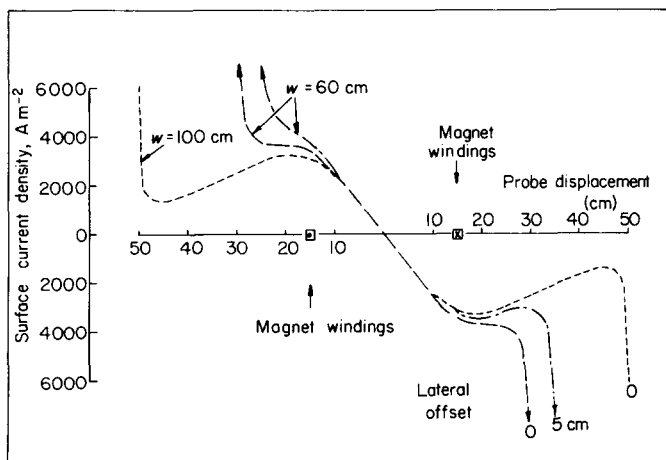


Fig. 7 The local induced eddy current density across levitation strips of width 1.0 m and 0.6 m due to a 50 turn magnet (100 cm long x 30 cm wide) with 0.2 A rms at 1 kHz, at a suspension height of 22 cm

results for strips of width 60 cm and 100 cm are shown in Fig. 7. High surface current densities are evident close to the edges, and these are responsible for the degradation in lift/drag ratio of the suspension and for the destabilizing forces experienced by the magnets when off-centre.

The results of a preliminary economic analysis of the levitation system are shown in Fig. 8. Operating costs (to overcome magnetic and aerodynamic drag) are added to a 12% write-off of the capital cost of guideway aluminium to give the total annual cost as a function of levitation strip thickness. The following data has been used:

- (a) A 300 kN Maglev vehicle travelling at 480 km h<sup>-1</sup> is levitated by 8 magnets, each 1.0 m long x 0.3 m wide, 0.22 m above aluminium strips 0.8 m wide. The degradation in lift/drag ratio compared with a wide sheet is taken as 20%.
- (b) The fabricated cost of aluminium is taken as 60 cents per lb, at a capital write-off rate of 12%. The cost of electric

energy is taken as 1 per cent per kW h<sup>-1</sup>, with an energy conversion efficiency of 50%.

- (c) The service rate is taken as 144 trips per day in each direction between Toronto and Montreal via Ottawa. The 594 km trip is scheduled to take 75 minutes.

While it might seem unrealistic to base an economic optimization of a system with an implementation time more than ten years hence on effectively 1975 prices, the position of the minimum cost in Fig. 8 is sensitive only to large relative changes in item costs. This optimization indicates that, for Canadian applications, the levitation conductor in high speed sections should be relatively thin, and a thickness of 1 cm is specified in our reference design.

The speed dependence of the operating characteristics (levitation height and drag) of the vehicle levitation system are shown in Fig. 9. The use of a 1 cm thick strip for low speeds would lead to excessive magnetic drag. Therefore, in pre-determined acceleration and deceleration sections, the strip thickness is graded from 1 cm to 3 cm to make the total drag force (aerodynamic and magnetic) and the levitation height almost speed independent. At very low speed, the vehicle is supported by wheels and levitation conductor is omitted from the guideway, thus avoiding the magnetic drag peak. A smooth transition onto the guideway conductor is achieved by means of a short aluminium ramp.

### Propulsion

The propulsion unit for the proposed Maglev vehicle must provide a maximum thrust of 70 kN to overcome aerodynamic and magnetic drag and for acceleration at about 0.1 g (set by passenger comfort consideration). Maximum power

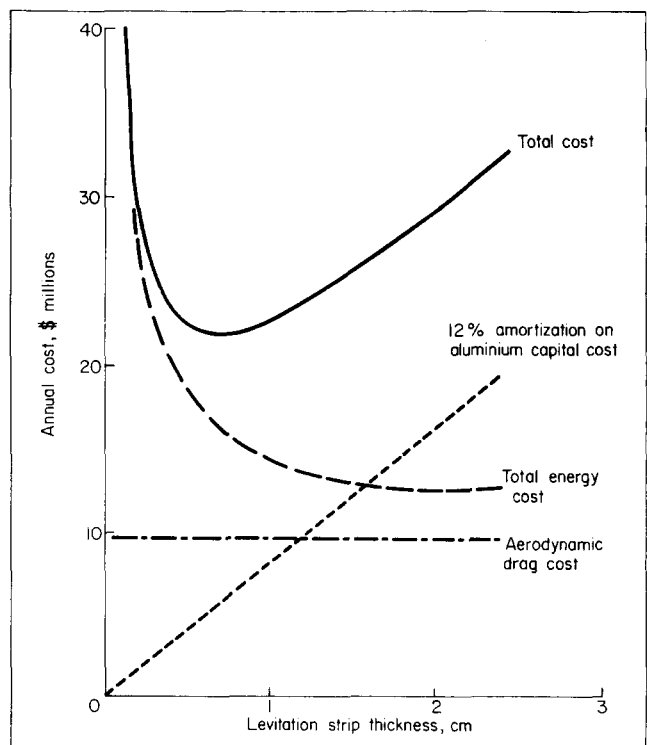


Fig. 8 The annual costs of energy and aluminium for levitation as a function of strip thickness for the proposed Canadian Maglev system

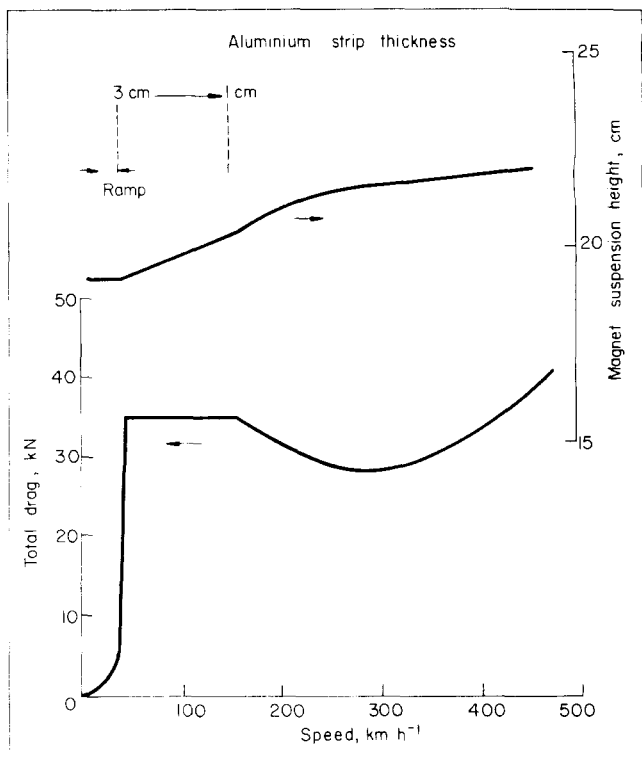


Fig.9 The levitation height and total drag (magnetic and aerodynamic) for a Maglev vehicle as functions of speed. Guideway aluminium is omitted below  $50 \text{ km h}^{-1}$  (on wheels), graded from 3 cm to 1 cm for  $50\text{--}160 \text{ km h}^{-1}$ , 1 cm thick above  $160 \text{ km h}^{-1}$

under acceleration is set at 8 MW, while cruising power (at  $480 \text{ km h}^{-1}$ ) is nominally 6 MW.

The linear synchronous motor has been selected as the most compatible with the electrodynamic suspension. Initial reactions to this proposal were that starting, efficiency and the high cost of the active guideway windings would all be serious problems. However, in each of these areas, analysis and modelling has proved very encouraging.

The variable speed LSM uses an array of fifty superconducting magnets of alternate polarity, mounted along the underside of the vehicle and powered split three-phase windings on the guideway, as shown in Fig.3. The length and pitch of the magnets have been carefully selected for nearly optimum efficiency at a suspension height of 22 cms,<sup>5,6</sup> while the magnet width is nearly the maximum allowable from vehicle layout considerations. The powered block length and winding conductor size, specified in Table 1, are set primarily by economic optimization between operating efficiency and capital cost.<sup>5</sup> Superconducting magnets enable a high efficiency (72%) to be achieved at a large clearance, while the LSM uses substantially less guideway conductor than is generally required for a linear induction motor reaction rail.

The guideway windings are powered by a variable frequency constant current inverter. A high power factor (0.82) is achieved by operating the motor at a current angle (the phase angle between 'field' and 'armature' currents) greater than  $90^\circ$ .<sup>5</sup> The resultant instability under open loop conditions must be controlled by continuously monitoring the current angle at the inverter. In this mode the LSM provides a small lift force, and current angle control can be used to damp heave motions of the vehicle (since the levitation system is inherently underdamped). Powering and controlling the

split three-phase windings independently could also be used to provide roll damping.

The use of an active guideway avoids the problems of high speed track side power collection. On-board power for passenger services is provided by a ram air turbine with auxiliary storage batteries for use at low speeds.

The LSM requires no vehicle-ground communications link. It is ideally suited to automatic system control, providing programmed acceleration, cruising, and deceleration, and can be used for precise vehicle location.

## Guidance

Experimental studies with full scale guideway sections exposed to the elements in Canadian winters have shown that ice and snow accumulation can be a serious problem for any configuration with vertically protruding parts (for example, channel and inverted tee designs). A flat-topped elevated guideway configuration has therefore been proposed.

It has been shown that the interaction between vehicle-borne magnets and either levitation strips or LSM windings (as shown in Fig.3) cannot alone provide adequate restoring forces.<sup>7</sup> The use of additional looped conductors in the guideway has therefore been examined.

One promising scheme involves the interaction between the propulsion magnets and flat null-flux loops mounted horizontally along the centre of the guideway, as shown in Fig.3. Analysis of the guidance characteristics of this scheme<sup>7</sup> shows that a lateral stiffness of  $10^6 \text{ N m}^{-1}$  can be achieved<sup>4</sup> for lateral displacements up to nearly 20 cm. The guidance force decreases for larger displacements, but can be reinforced by the interaction of the propulsion magnets with the edges of the levitation strips. The position dependence of both contributions to the guidance force is shown in Fig.10. A total restoring force equal to the vehicle weight ( $300 \text{ kN}$ ) is developed at a displacement of 30 cm ( $100 \text{ km h}^{-1}$  side wind is estimated to produce a side force of  $70 \text{ kN}$ ).

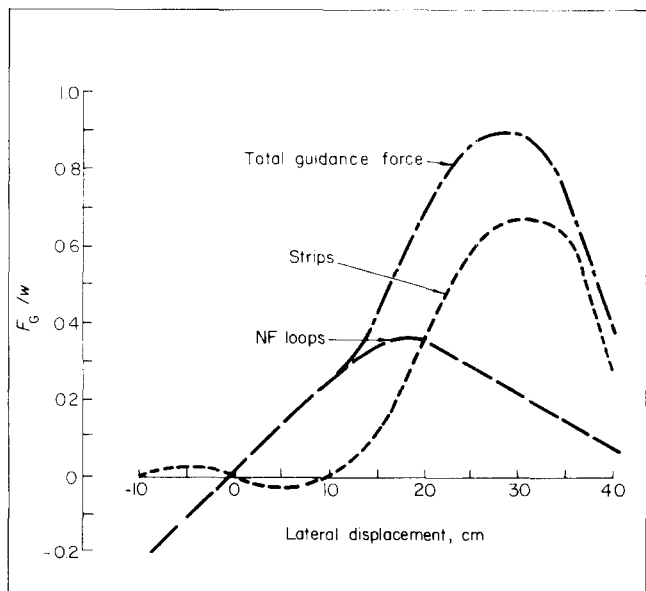


Fig.10 Guidance force (determined by impedance modelling and normalized to a vehicle weight of  $300 \text{ kN}$ ) as a function of lateral displacement for the interaction between LSM magnets and both null-flux loops and the levitation strip edges (see Fig.3)

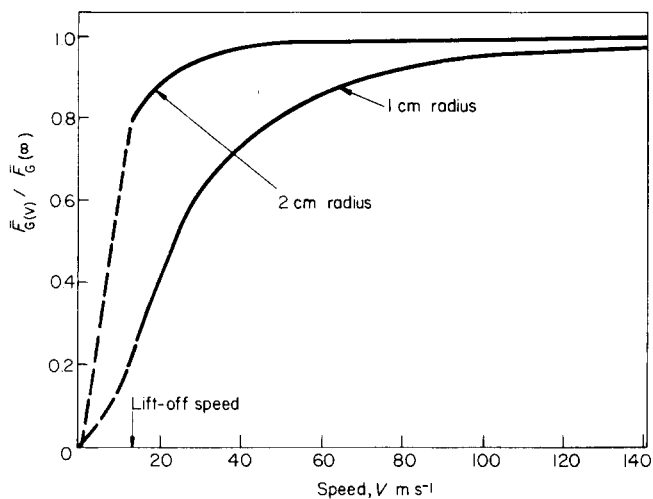


Fig. 11 The mean guidance force, normalized to its high speed limit, for an array of LSM magnets moving over null-flux loops of different conductor radii, as a function of speed

Along high speed sections of the guideway, the overall radius of the null-flux loop conductor, stranded to minimize parasitic eddy current losses, would be 1 cm. High guidance forces (over 80% of the high speed stiffness) can be maintained to the levitation touch-down speed of 45 km h<sup>-1</sup> by increasing the conductor radius to 2 cm along pre-determined low speed sections. The speed dependence of the null-flux guidance force is shown in Fig. 11.

We are continuing to study alternative flat guidance schemes. The null-flux system favoured at present produces strong guidance forces at all speeds that the vehicle is levitated with low power dissipation (130 kW for a 30 kN guidance force) occurring only when the vehicle is displaced laterally.

### Cryogenics

For fail-safe operation, each of the eight levitation magnets would use a separate cryogenic support system. Using compressed superinsulation supports, and a single intermediate temperature shield, refrigeration requirements for each levitation magnet are calculated as about 2½ W (primarily due to the load bearing material transmitting the levitation force). For cryogenic purposes, the fifty LSM magnets would be divided into ten groups, each of five magnets. Each group would have a similar refrigeration requirement to that of a single levitation magnet (because the larger surface area is balanced by the lower forces).

Total heat leak to the superconducting magnets on the Maglev vehicle is therefore estimated to be 45 W. The three refrigeration techniques examined were:

(a) Open bath — rejected because approximately 500 million ft<sup>3</sup> per year of helium gas would be lost to the atmosphere for a Maglev system in Canada alone. This is comparable with the current total annual helium usage for all applications. Although this is a simple system which minimizes the weight of on-board refrigeration components, it is unlikely to be economical and is unacceptable since helium is a disappearing natural resource.

(b) On-board refrigeration — one small refrigerator for each levitation magnet and for each group of propulsion magnets was considered in order to minimize cryogenic

pipng. This system is not favoured because of its many disadvantages — weight of the helium compressors, additional on-board power requirements, and reliability and maintenance considerations.

(c) Isochoric (sealed) dewar operation<sup>8</sup> — the helium vessel around each levitation magnet or group of propulsion magnets would be coupled to a 100 l helium reservoir. A 75 l nitrogen reservoir would supply intermediate temperature refrigeration for the entire vehicle. The helium space would be sealed and during the operating day the heat leak would cause the temperature and pressure to rise. At night the pressurized gas would be discharged to a ground-based refrigerator and the dewars recharged with liquid helium at 4.2 K.

Fig. 12 shows the temperatures and pressures resulting from heat inputs, in terms of watt hours per litre of dewar capacity, as functions of the percentage fill of liquid helium at atmospheric pressure. It will be noted that:

- (i) the liquid fill should be between 50% and 80% of capacity,
- (ii) for a 22 hour 2½ W heat leak to a 100 l reservoir, the heat input of 0.55 Wh l<sup>-1</sup> would generate maximum pressure and temperature of about 20 atm and 13 K,
- (iii) Nb<sub>3</sub>Sn (or higher T<sub>c</sub>) superconductor should be used in order to retain reasonable working current densities at the higher temperatures.

The mass of all the pressurized storage reservoirs is estimated to be about 700 kg, including cryogenic liquids. Isochoric dewar operation is therefore both lightweight and simple, and appears to be the cryogenic support system best suited for Maglev vehicles.

### Test programme

The Canadian test programme uses a 7.6 m diameter wheel, rotating about a vertical axis with a maximum peripheral speed of 100 km h<sup>-1</sup>, to perform full-scale tests of the propulsion, levitation, and guidance systems. Conductor configurations are attached to the outer rim, and their interactions with stationary full-scale superconducting magnets are measured.

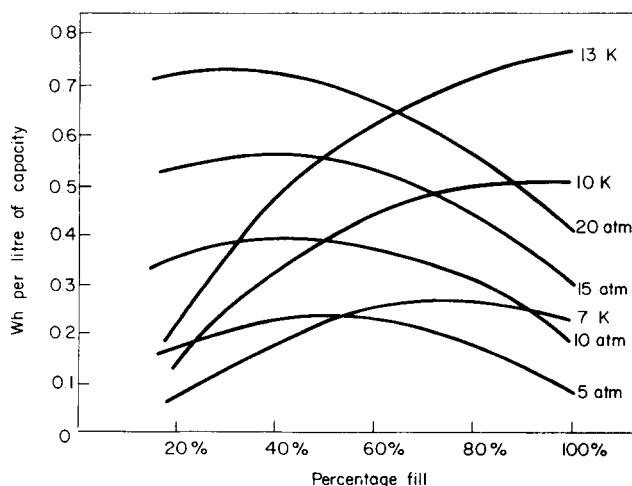


Fig. 12 The temperature and pressure resulting from heat inputs, in terms of Wh l<sup>-1</sup> of dewar capacity, as a function of percentage fill of liquid helium at atmospheric pressure

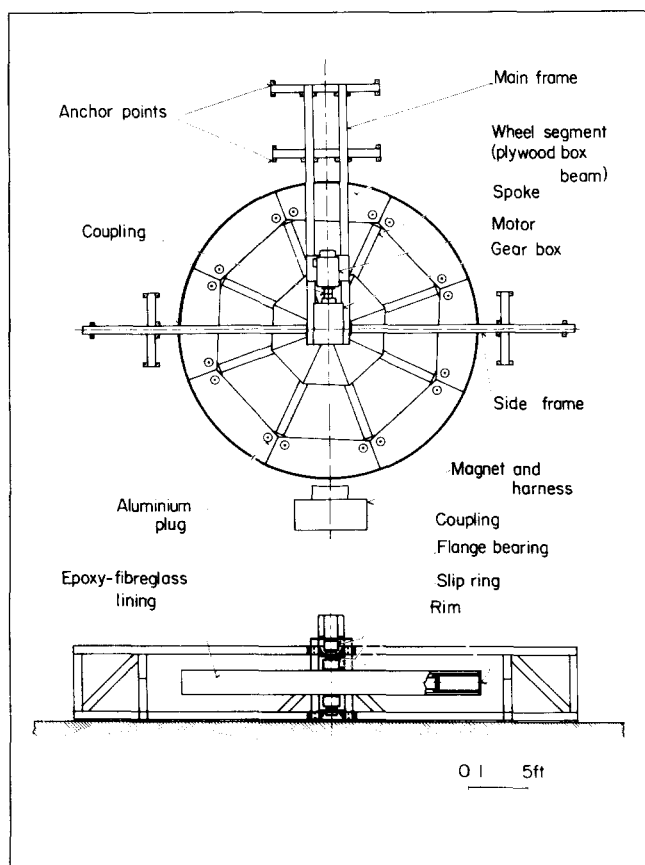


Fig.13 Plan and side views of the test wheel

A rotating wheel type test facility has been chosen in order to investigate a wide variety of guideway configurations. Speeds have been restricted to  $100 \text{ km h}^{-1}$  in order to use full-scale superconducting magnets and guideway configurations. Speed effects in the range  $100\text{--}480 \text{ km h}^{-1}$  are readily extrapolated.

The test wheel, shown in Fig.13, resembles a large cartwheel on the rim of which guideway components can be mounted. The vertical steel shaft and hub are supported in two flanged roller bearings, attached to the upper and lower portions of the square-section steel framework. Eight reinforced aluminium I beams form the spokes. The rim of the wheel is made of eight plywood box-beam segments, and a wrap of epoxy prepregated fibre-glass cloth, wound under tension and cured by an array of infra-red lamps, forms an outer 'tyre'.

The wheel can be driven by a 1 750 rpm variable speed 150 hp dc motor through a 25:1 spiral bevel gearbox. Speed control is obtained through a thyristor power supply.

Experimental work requires the measurement of forces and moments developed on the superconducting magnets. A magnet harness is being constructed to support either propulsion or levitation magnet dewars and to measure lift, propulsion/drag and lateral forces, and pitch, roll and yaw moments. The system will allow lateral, vertical, and three orthogonal angular adjustments. Meanwhile a simplified magnet support system allowing the measurement of propulsion/drag and normal forces is being used.

The first phase of the experimental programme involves testing the LSM. Full scale split three-phase LSM windings,

formed from 1 cm diameter stranded aluminium cable, on a 52 cm pitch are positioned on the rim and covered with a wrap of fibre-glass roving in order to withstand the 21 g centrifugal forces. The windings are powered by a three-phase variable frequency, 50 kVA inverter through slip rings mounted on the drive shaft. The resultant travelling field interacts with a single stationary full scale superconducting propulsion magnet to drive the wheel.

The LSM propulsion test magnet is an interim version using readily available conductor, and has been designed to run at  $3 \times 10^5$  ampere-turns (rather than  $5 \times 10^5$  ampere-turns specified for the operational LSM).

The magnet is mounted in the close fitting tail section of a massive nitrogen shielded stainless steel dewar with upper helium and nitrogen reservoirs. The lower end of the helium container, through which the magnet was introduced, was sealed by a base plate with compressed indium. This proved troublesome and prone to leakage when cold, causing delays to the tests, and was later replaced by a soldered seal.

The magnet has been tested and performs well with no quenches or evidence of instability up to a level of about  $2.3 \times 10^5$  ampere-turns (corresponding to a supply current of 900 A). Above this level, the magnet has been quenched on several occasions (at currents of 900–1150 A) without damage. The first phase of the LSM tests, involving demonstration of starting and acceleration with a large scale LSM, measurement of basic motor characteristics and forces, and operation with phase angle control, has now been successfully completed. The results are in good agreement with analytical work<sup>9</sup> at the University of Toronto and will be reported in detail elsewhere.

## Discussion

The principles of magnetic levitation and propulsion have been well known for over a half century. The new technologies of superconducting magnets, high power semiconductor switches, inverters etc, now enable the early ideas to be exploited. Electrodynamic suspension and linear synchronous motor propulsion have been demonstrated at essentially full scale, and the analytical tools to handle realistic configurations have recently become available.

The major problems appear to be demonstrating the reliability of vehicle-borne superconducting magnets and cryogenics (for the uninitiated), and the dynamic response of the system, reflected in ride quality. The suspension is inherently under-damped and some form of active control in the system is probably required. Independent phase angle control of the split three-phase windings of the LSM can damp heave, yaw, and roll motions, but may not be adequate for all coupled modes.

Superconducting magnetic levitation and linear synchronous motor propulsion are now being recognized as the most promising technologies for HSGGT. However, as indicated by the diversity of system proposals, we are still in the conceptual design phase. It is likely that configurational distinctions, optimized to different applications, will persist through the development stage.

Any inter-city transit system is expensive and is rightly the subject of public and political debate. In order to be a serious contender a new scheme must proceed through the design, development, and demonstration stages, involving an expenditure equal to a small percentage of the final cost. This could

well exceed \$100 000 000, and Maglev expenditures throughout the world have yet to reach this figure. Emphasis on environmental impact, the economic situation, transportation demand, energy policies, and public and political sentiments will all affect the pace of future development.

This work is supported by the Transportation Development Agency and by the National Research Council through the Canadian Institute of Guided Ground Transport.

## References

- 1 Data taken from; 'Intercity passenger transport study', Canadian Transport Commission Research Branch, Cat No TT22-1/1970
- 2 Ooi, B. T., Eastham, A. R. *IEEE Trans on Power Apparatus and Systems PAS-94* (1975) 72
- 3 Atherton, D. L., Eastham, A. R., Fombrun, C., Chong, M. *Can J Phys* 52 (1974) 1203
- 4 Atherton, D. L., Eastham, A. R. *IEEE Trans on Magnetics MAG-10* (1974) 413
- 5 Slemmon, G. R., Burke, P. E., Turton, R. A. *IEEE Trans on Magnetics MAG-10* (1974) 435
- 6 Atherton, D. L., Love, L. E. G., Prentiss, P. O. *Can J Phys* 50 (1972) 3143
- 7 Atherton, D. L., Eastham, A. R. *J Appl Phys* 45 (1974) 1398
- 8 Ishizaki, Y., Kuroda, R., Ohtsuka, T. Proc ICECS (IPC Science & Technology Press Ltd, UK) 102
- 9 Canadian Maglev Group, Annual Report (1975) Project No D-71-72: available from CIGGT, Queen's University

## Corrigenda

Vol 14 No 7 'Contact resistance in liquid nitrogen'  
A. Kawashima and S. Hoh

Page 381 1st column, last line

Units of contact resistance should be m Ω not mm Ω

Page 382 Fig.2 and page 383, Fig.8

Units of ordinate should be m Ω not mm Ω

Vol 14 No 11 'New forms of state equations of helium'  
V. Arp

Page 593 equation 1 should read

$$TI(P, H) = \frac{2H}{5R} - (2.8239 + 0.64469P - 5.615 \times 10^{-6} P^2)$$

equation 4 should read

$$HI(P, S) = 3.6785757 P^{0.4} \exp\left(\frac{S - 0.0001077 P}{2.5 R}\right)$$

$$+ 14.6649 + 0.33479 P - 0.00002913 P^2$$

Page 595 3rd paragraph, 5th line should read

between 10 and 15 K is an overlap region between two separate mathematical functions ...

Page 596 1st column, 1st equation should read

$$T^* = TI(P, H) + P \sum_{i=1}^6 \delta_i t^i + (1+h^2)^{-1} \sum_{i=1}^5 \delta_{6+i} P^{0.2i} + (1+h^4)^{-1} \sum_{i=0}^4 \sum_{j=0}^5 \left(\frac{1}{h}\right)^{i/2} P^{0.2j}$$

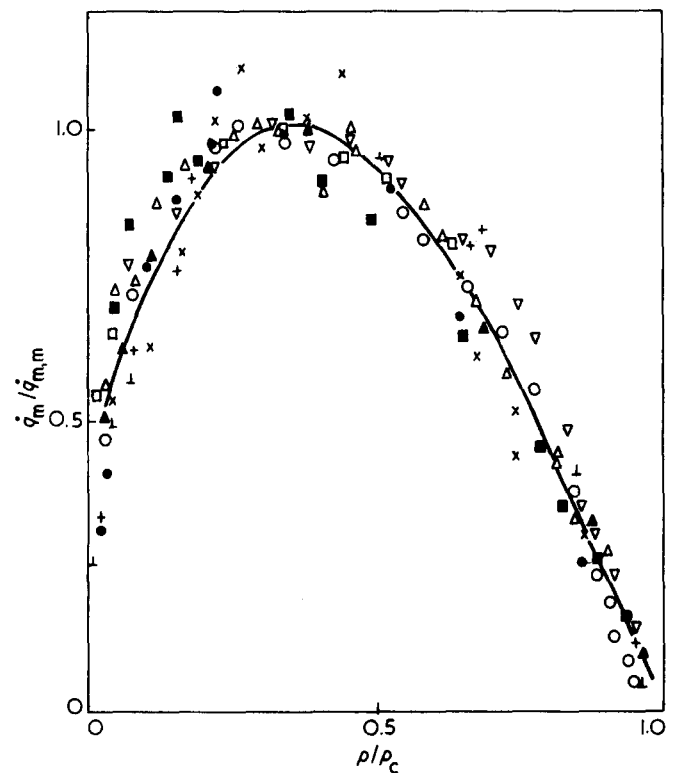
Page 598 Table 3, 2nd column, 1st line should read

$$c_{44} = -90.187334672$$

Vol 15 No 3 'Heat transfer in cryogenic liquids under pressure'

L. Bewilogua, R. Knöner, and H. Vinzelberg

Page 125 Fig.9 Some of the symbols were not reproduced correctly. The correct version is shown below.



Vol 15 No 3 'Reducing constants for corresponding states and reduced equations of state'

E. M. Holleran

Page 137 2nd column, 2nd paragraph, line 2 should read

this system may be written as  $Z = Z(\theta, \delta)$

Page 139 equation 7 should read

$$Z = Z(\theta, \delta, C_3)$$

Vol 15 No 4 'A correlation of critical points'

E. M. Holleran, R. E. Walker, and C. M. Ramos

Page 216 5th paragraph, 2nd sentence should read

For example, two different sets of PVT data for neon<sup>13,31</sup> gave  $k_B$ ,  $T_B$ ,  $d_o$  values of 2.09, 115.3 K, 90.1 m l<sup>-1</sup>, and 1.90, 119.2K, 86.4 m l<sup>-1</sup>.